

# Halogen Oxidation of Tetrakis(dithioacetato)diplatinum(II) Complexes, $Pt_2(CH_3CS_2)_4$ . Synthesis and Characterization of $Pt_2(CH_3CS_2)_4X_2$ ( $X = Cl, Br, I$ ) and Structural, Electrical, and Optical Properties of Linear-Chain ( $\mu$ -Iodo)tetrakis(dithioacetato)diplatinum, $Pt_2(CH_3CS_2)_4I$

CARLO BELLITTO,\* ALBERTO FLAMINI,\* LEONARDO GASTALDI,\* and LUCIO SCARAMUZZA

Received February 25, 1982

The halogen oxidation reaction of tetrakis(dithioacetato)diplatinum(II) has been investigated. Compounds having the formula  $Pt_2(CH_3CS_2)_4X_2$  ( $X = Cl, Br, I$ ), with formal oxidation number +3, have been synthesized and characterized. They are diamagnetic and consist of dimeric  $Pt_2S_8X_2$  units. In the case of  $X = I$ , if the reaction is carried out with  $Pt:I = 1:0.5$ , another product, having the formula  $Pt_2(CH_3CS_2)_4I$ , with formal oxidation state +2.5, is isolated. The X-ray structure consists of linear chains of  $\cdots Pt_2S_8 \cdots I \cdots Pt_2S_8 \cdots I \cdots$ , stacking along the crystallographic  $b$  axis (monoclinic space group  $C2/c$ ). The Pt-Pt distance in the dimer is 2.677 (2) Å, and the Pt-I distances are respectively 2.975 (1) and 2.981 (3) Å. This is the first example, as far as we know, of a linear-chain compound having dimeric  $[Pt_2S_8]$  chromophores bridged through halides with a nearly symmetrical metal-halogen-metal bridge. The maximum powder electrical conductivity at 300 K is  $7 \times 10^{-3} \Omega^{-1} \text{cm}^{-1}$ . Variable-temperature studies show that, over the range investigated, the electrical conductivity follows an exponential temperature dependence with a very low activation energy, 0.05 eV. A "hopping-type" mechanism seems to be responsible for the electrical conductivity.

## Introduction

One-dimensional materials are the object of intense interest on the part of chemists and physicists because they show spectacular and highly anisotropic electrical, magnetic, and optical properties.<sup>1</sup> Most of the 1-D electrically conductive complexes studied to date contain infinite stacks of planar molecules and nonintegral formal oxidation number of the constituents,<sup>2</sup> but only a few of them show "metallic behavior".<sup>3</sup> Chain structure is therefore the first requisite for obtaining such behavior.

Recently, we found that several nickel-triad metal(II) derivatives of dithiocarboxylato ligands crystallize in a columnar structure, with either dimeric or monomeric units. The dithioacetato palladium(II) complex, for example, exists in two solid-state phases.<sup>4</sup> The first one contains a one-dimensional arrangement of dimeric molecules with  $CS_2$  incorporated between the columns. The second one consists of mononuclear and binuclear units, alternating along the  $a$  axis of the unit cell. On the other hand, the dithioacetato platinum(II) complex crystallizes in dimeric units,  $Pt_2(CH_3CS_2)_4$ , stacking in columns along the crystallographic  $c$  axis.<sup>5</sup>

In an attempt to obtain further analogues with sulfur-containing ligands having nonintegral formal oxidation state, and possibly with "metallic behavior", we studied the reaction of dithiocarboxylato derivatives of Pt(II) and Pd(II) with halogens. Here we report the synthesis and chemical and physical properties of complexes obtained by reaction of halogens with tetrakis(dithioacetato)diplatinum(II) and the crystal structure of the mixed-valence ( $\mu$ -iodo)tetrakis(dithioacetato)diplatinum.

## Experimental Section

Elemental analyses were performed by Alfred Bernhardt Mikroanalytische Laboratorium, Elbach, West Germany.

**Reagents.** Dithioacetic acid,  $CH_3CS_2H$ , was prepared according to known procedures.<sup>6</sup>  $K_2PtCl_4$  was used as obtained from B.D.H. Chemicals Ltd. Tetrakis(dithioacetato)diplatinum(II),  $Pt_2(CH_3CS_2)_4$ ,

was prepared as reported previously,<sup>4</sup> and the purity was checked by normal physicochemical methods. Halogens were used as obtained commercially without further purification.

**Synthesis of  $Pt_2(CH_3CS_2)_4X_2$  Complexes ( $X = Cl, Br, I$ ).**  $Pt_2(CH_3CS_2)_4Cl_2$ .  $Pt_2(CH_3CS_2)_4$  (0.300 g,  $4 \times 10^{-4}$  mol) was dissolved in hot toluene (200 mL) until a clear red-orange solution was obtained. The  $Cl_2$  gas was bubbled into the solution. Immediately a brown microcrystalline product separated. The product (0.300 g, 92% yield) was collected, washed with toluene, and dried under vacuum. Anal. Calcd for  $C_8H_{12}S_8Pt_2Cl_2$ : C, 11.64; H, 1.45; S, 31.06; Pt, 47.26; Cl, 8.59. Found: C, 11.58; H, 1.31; S, 30.78; Pt, 46.97; Cl, 8.56.

$Pt_2(CH_3CS_2)_4Br_2$ .  $Pt_2(CH_3CS_2)_4$  (0.349 g,  $4.6 \times 10^{-4}$  mol) was dissolved in hot toluene (200 mL). A chloroform solution of  $Br_2$  (10 mL, 0.5% in volume) was added dropwise to the complex solution. A red-orange microcrystalline product separated immediately. The compound was collected, washed with toluene, and dried under vacuum (0.377 g, 90% yield). Anal. Calcd for  $C_8H_{12}S_8Pt_2Br_2$ : C, 10.50; H, 1.31; S, 28.04; Pt, 42.66; Br, 17.47. Found: C, 10.39; H, 1.23; S, 27.88; Pt, 42.49; Br, 17.69.

$Pt_2(CH_3CS_2)_4I_2$ .  $Pt_2(CH_3CS_2)_4$  (0.350 g,  $4.6 \times 10^{-4}$  mol) was dissolved in hot toluene (200 mL). Iodine (0.126 g,  $5 \times 10^{-4}$  mol), dissolved in toluene (20 mL), was added dropwise. A dark violet microcrystalline product precipitated (0.430 g, 95% yield). Anal. Calcd for  $C_8H_{12}S_8Pt_2I_2$ : C, 9.53; H, 1.19; S, 25.43; Pt, 38.68; I, 25.16. Found: C, 9.63; H, 1.03; S, 25.31; Pt, 38.87; I, 24.97.

**Synthesis of  $Pt_2(CH_3CS_2)_4I$ .** The above reaction carried out with a ratio  $Pt:I = 1:0.5$  gave needlelike dark violet crystals in quantitative yield. Suitable crystals for X-ray studies were grown from a porous frit in which the iodine solution was allowed to diffuse inside a hot toluene solution of  $Pt_2(CH_3CS_2)_4$  under nitrogen. It was later discovered that the title compound can be obtained from the reaction of  $Pt_2(CH_3CS_2)_4$  with  $Pt_2(CH_3CS_2)_4I_2$  in toluene at reflux. Anal. Calcd for  $C_8H_{12}S_8Pt_2I$ : C, 10.89; H, 1.36; S, 29.09; Pt, 44.25; I, 14.39. Found: C, 10.95; H, 1.42; S, 28.93; Pt, 44.03; I, 14.16.

**Physical Measurements. Infrared Spectra.** Routine IR spectra were recorded with a Perkin-Elmer 621 spectrophotometer on KBr pellets.

**Electronic Spectra.** Solution and solid-state spectra were recorded on a Cary 14 spectrophotometer. The compounds were diluted in KBr and studied as KBr pellets.<sup>7</sup> Low-temperature measurements were obtained with use of an Oxford Instruments C.F. 100 cryostat adapted for the Cary 14; liquid  $N_2$  was used as the cooling liquid. A Beckman DK-2A was used to record diffuse-reflectance spectra on  $MgO$ -diluted samples.

**Thermogravimetric Measurements.** Differential scanning calorimetry (DSC) and thermal gravimetric analyses (TGA) were performed with a Du Pont 950 apparatus.

- (1) Miller, J. S.; Epstein, A. J., Eds. *Ann. N.Y. Acad. Sci.* **1978**, *313*, 1-828.
- (2) Krogmann, K. *Angew. Chem., Int. Ed. Engl.* **1969**, *8*, 35.
- (3) Underhill, A. E.; Watkins, D. M. *Chem. Soc. Rev.* **1980**, 429.
- (4) Bellitto, C.; Flamini, A.; Piovesana, O.; Zanazzi, P. F. *Inorg. Chem.* **1979**, *18*, 2258.
- (5) Bellitto, C.; Flamini, A.; Piovesana, O.; Zanazzi, P. F. *Inorg. Chem.* **1980**, *19*, 3632.
- (6) (a) Houben, J.; Pohl, H. *Chem. Ber.* **1907**, *40*, 1907. (b) Beiner, J. M.; Thuillier, A. *C.R. Hebd. Seances Acad. Sci., Ser. C* **1972**, *274*, 642.

(7) Wroblewski, J. T.; Long, G. J. *J. Appl. Spectrosc.* **1977**, *31*, 177.

**Table I.** Fractional Atomic Coordinates and Thermal Parameters for Non-Hydrogen Atoms of  $\text{Pt}_2(\text{CH}_3\text{CS}_2)_4\text{I}^a$ 

atoms	x	y	z	$U_{11}$	$U_{22}$	$U_{33}$	$U_{23}$	$U_{13}$	$U_{13}$
Pt(1)	0.0	0.4098 (1)	0.25	327 (7)	271 (6)	239 (7)	0	75 (6)	0
Pt(2)	0.0	0.0997 (1)	0.25	341 (1)	265 (6)	259 (7)	0	118 (6)	0
I(1)	0.0	0.7551 (4)	0.25	570 (13)	601 (14)	642 (14)	0	241 (11)	0
S(1)	0.1289 (4)	0.4212 (6)	0.2206 (5)	369 (26)	325 (23)	414 (30)	17 (22)	137 (24)	9 (21)
S(2)	0.0923 (4)	0.0884 (6)	0.1558 (5)	527 (33)	344 (23)	467 (32)	-67 (25)	269 (28)	-50 (26)
S(3)	0.0713 (4)	0.4217 (6)	0.4283 (4)	503 (32)	372 (25)	278 (24)	-79 (20)	69 (24)	31 (25)
S(4)	0.1108 (4)	0.0846 (6)	0.4043 (4)	466 (30)	338 (23)	327 (26)	75 (22)	68 (24)	47 (25)
C(1)	0.1437 (12)	0.2569 (24)	0.1641 (14)	434 (73)	315 (64)	382 (69)	63 (79)	218 (60)	36 (81)
C(2)	0.2177 (14)	0.2589 (31)	0.1252 (18)	450 (79)	718 (91)	589 (84)	164 (92)	302 (70)	220 (88)
C(3)	0.1203 (12)	0.2513 (26)	0.4700 (13)	532 (77)	337 (63)	256 (62)	143 (76)	193 (59)	-75 (83)
C(4)	0.1808 (14)	0.2537 (28)	0.5824 (15)	538 (82)	480 (76)	331 (70)	-100 (87)	73 (67)	189 (87)

<sup>a</sup> The esd's in parentheses refer to the last digit.

**X-ray Photoelectron Spectroscopy.** XPS spectra were recorded on a V.G. Esca 3 Mk II instrument using Al K $\alpha$  (1486.6 eV) radiation, located at the Servizio ESCA of the Area Ricerca di Roma, CNR. As a check for possible loss of iodine from  $\text{Pt}_2(\text{CH}_3\text{CS}_2)_4\text{I}_x$  ( $x = 1, 2$ ) in the high-vacuum chamber of the spectrometer, the I 3d $_{5/2}$  peak was recorded at the beginning and at the end of each run; no drop of the intensity of this peak was observed. Samples were dusted on a double-sided adhesive tape. Binding energies reported are relative to the C 1s peak (285.0 eV) from the tape used as reference.

**Mass Spectra.** Mass spectra were recorded with a V.G. 70-70 F double-focusing mass spectrometer at an ionizing voltage of 70 V of the Mass Spectra Service, Area Ricerca di Roma, CNR. The sample temperature ranged between 140 and 240 °C. Samples were introduced into the ionization chamber via the direct-insertion lock. Perfluorokerosene was used as a mass reference.

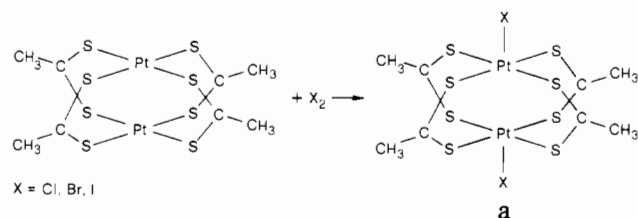
**Magnetic Measurements.** The static susceptibility,  $\chi$ , was measured by the Gouy method, with use of  $\text{Hg}(\text{Co}(\text{SCN})_4)$  as standard. EPR spectra were obtained with an X-band Varian E-9 spectrometer. DPPH ( $g = 2.0036$ ) was used as reference for measuring the  $g$  values. EPR spectra at 4.2 and 77 K were recorded with use of an Oxford Instruments C.F. ESR 9 cryostat.

**Electrical Conductivity Measurements on Polycrystalline Samples.** Electrical conductivity data on polycrystalline  $\text{Pt}_2(\text{CH}_3\text{CS}_2)_4\text{I}$  were acquired with a four-probe van der Pauw method.<sup>8</sup> Samples were prepared by pressing powders under 6 kbar pressure into cylindrical pellets, 12 mm in diameter and 1 mm in thickness. Pellets were mounted with four fine gold wires, and electrical contacts were made with Du Pont silver paint (No. 4929). The current for dc conductivity measurements was supplied by a Keithley Model 225 regulated current source; voltage was measured on a Keithley Model 173 multimeter. Variable-temperature measurements were made with use of an Oxford Instruments modified C.F. 100. The temperature was monitored with a C.L.T.S. sensor.

**Crystal Data and Intensity Measurements.**  $\text{Pt}_2(\text{CH}_3\text{CS}_2)_4\text{I}_2$ . Since we have not yet succeeded in growing crystals suitable for X-ray analysis, here we report only preliminary X-ray data. From Weissenberg and oscillation photographs the compound crystallizes in an orthorhombic space group with unit-cell dimensions  $a = 9.84 \text{ \AA}$ ,  $b = 13.30 \text{ \AA}$ , and  $c = 8.04 \text{ \AA}$ .

**$\text{Pt}_2(\text{CH}_3\text{CS}_2)_4\text{I}$ .** A needle-shaped crystal of dimensions  $0.30 \times 0.08 \times 0.08 \text{ mm}^3$  was selected and mounted on a glass capillary. Preliminary oscillation and Weissenberg photographs showed the ( $h0l$ ) reflections were absent for  $l \neq 2n$ , suggesting the space group to be  $C2/c$  or  $Cc$ ; further investigations confirmed the former group. The cell dimensions obtained by least-squares refinement of setting angles of 15 reflections measured on a Syntex P2 $_1$  four-circle diffractometer with graphite-monochromatized Mo K $\alpha$  radiation ( $\lambda = 0.71073 \text{ \AA}$ ) are  $a = 16.838 (4) \text{ \AA}$ ,  $b = 8.633 (2) \text{ \AA}$ ,  $c = 13.635 (4) \text{ \AA}$ ,  $\beta = 109.39 (5)^\circ$ , and  $V = 1869.5 \text{ \AA}^3$ . The formula weight is 881.74 ( $\text{Pt}_2\text{C}_8\text{H}_{12}\text{S}_8\text{I}$ ), and  $D_c = 3.09 \text{ g cm}^{-3}$  for  $Z = 4$ . The absorption coefficient for Mo K $\alpha$  is  $198.7 \text{ cm}^{-1}$ . Intensity data were collected by the  $\omega$ - $2\theta$  scan technique in the range  $3^\circ \leq 2\theta \leq 60^\circ$ . The intensities of two reference reflections collected after 60 reflections were measured. Data were corrected for the Lorentz-polarization factors.

**Structure Solution and Refinement.** The structure was solved with use of the SHELX program system,<sup>9a</sup> in which a Patterson map yielded

**Scheme I****Table II.** Main Interatomic Distances in  $\text{Pt}_2(\text{CH}_3\text{CS}_2)_4\text{I}$  (Å)<sup>a</sup>

Pt(1)-Pt(2)	2.677 (2)	S(1)-C(1)	1.67 (2)
Pt(1)-I(1)	2.981 (3)	S(2)-C(1)	1.68 (2)
Pt(1)-S(1)	2.337 (6)	S(3)-C(3)	1.69 (2)
Pt(1)-S(3)	2.329 (6)	S(4)-C(3)	1.68 (2)
Pt(2)-I(1')	2.975 (3)	C(1)-C(2)	1.51 (3)
Pt(2)-S(2)	2.324 (6)	C(3)-C(4)	1.53 (3)
Pt(2)-S(4)	2.306 (6)		

<sup>a</sup> The esd's in parentheses refer to the last digit.

the positions of Pt and I atoms. The remaining non-hydrogen atoms were found by Fourier methods. All the atoms were assumed to be uncharged; the scattering factors and corrections for anomalous scattering for the listed final structure factors were taken from ref 9b. Isotropic full-matrix least-squares refinement led to an  $R$  of 0.09. Introduction of anisotropic temperature factors gave the final value of  $R$  of 0.050 for the 1200 independent observed reflections ( $R_w = 0.055$ ). The quantity minimized was  $\sum w(|F_o| - |F_c|)^2$  with the final weighting scheme  $w = 0.9637/[\sigma(F)^2 + 0.003179F_o^2]$ .

## Results

Tetrakis(dithioacetato)diplatinum(II) readily undergoes oxidative addition with halogens, giving compounds of formula  $\text{a}$  (Scheme I) containing platinum atoms with formal oxidation state +3. The formulation of  $\text{a}$  is based on the elemental analysis and IR spectra. Differential thermal analysis (DSC) and thermogravimetric analysis (TGA) measurements of the compounds show no phase transitions below the melting point, and they all melt with decomposition. They are completely insoluble in polar solvents and sparingly soluble ( $5 \times 10^{-5} \text{ M}$ ) in toluene and in dichloromethane, giving air-stable solutions. That  $\text{Pt}_2(\text{CH}_3\text{CS}_2)_4\text{X}_2$  compounds have a dimeric structure is suggested by the vibrational spectra. These are superimposable on those of  $\text{Pt}_2(\text{CH}_3\text{CS}_2)_4^5$  and  $\text{Pd}_2(\text{CH}_3\text{CS}_2)_4^4$ , compounds where the dimeric structure has been established. No Pt-S and Pt-X bands could be observed in the KBr region. In the case of X = iodine, if the reaction is carried out with a ratio Pt:I = 2:1, another product, having the formula  $\text{Pt}_2(\text{CH}_3\text{CS}_2)_4\text{I}$ , is isolated with platinum atoms in the formal

(8) Cahen, D.; Hahn, J. R.; Anderson, J. R. *Rev. Sci. Instrum.* **1973**, *44*, 1567.

(9) (a) Sheldrick, G. M. "The SHELX Program System"; University Chemical Laboratory: Cambridge, England, 1976. (b) "International Tables for X-ray Crystallography"; Kynoch Press: Birmingham, England, 1974; Vol. IV.

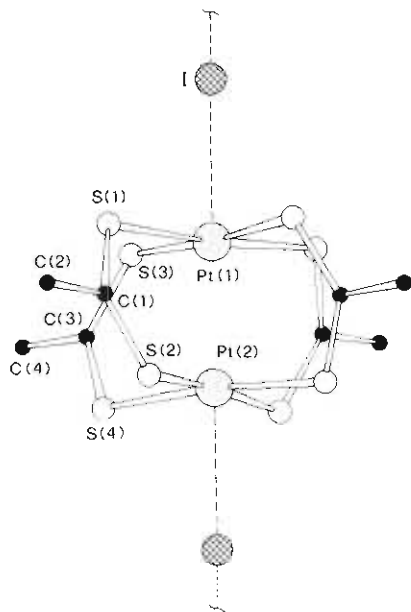


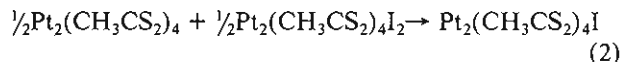
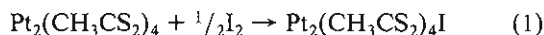
**Figure 1.** Atomic arrangement of  $\text{Pt}_2(\text{CH}_3\text{CS}_2)_4\text{I}$  along the twofold axis.

**Table III.** Main Interatomic Angles (deg) in  $\text{Pt}_2(\text{CH}_3\text{CS}_2)_4\text{I}^a$

S(1)-Pt(1)-S(3)	89.5 (2)	S(1)-C(1)-S(2)	128.0 (1.1)
S(2)-Pt(2)-S(4)	90.8 (2)	S(1)-C(1)-C(2)	114.8 (1.7)
Pt(1)-S(1)-C(1)	109.4 (7)	S(2)-C(1)-C(2)	117.0 (1.7)
Pt(1)-S(3)-C(3)	109.7 (7)	S(3)-C(3)-S(4)	128.2 (1.1)
Pt(2)-S(2)-C(1)	110.5 (7)	S(3)-C(3)-C(4)	114.3 (1.5)
Pt(2)-S(4)-C(3)	110.1 (7)	S(4)-C(3)-C(4)	117.4 (1.5)

<sup>a</sup> The esd's in parentheses refer to the last digit.

oxidation state +2.5. The new compound can be obtained by following either reaction 1 or reaction 2. The TGA and DSC



traces of the less iodinated complex show the one-stage iodine loss correspondingly to one iodine atom per molecule before decomposition. This compound is almost insoluble in nonpolar solvents and completely insoluble in the polar ones.

**Description of the Structure of  $\text{Pt}_2(\text{CH}_3\text{CS}_2)_4\text{I}$ .** Structural information on ( $\mu$ -iodo)tetrakis(dithioacetato)diplatinum is reported in Tables I-III and Figures 1 and 2. The crystal structure consists of chains of  $\text{---Pt}_2(\text{CH}_3\text{CS}_2)_4\text{---I---Pt}_2(\text{CH}_3\text{CS}_2)_4\text{---I---}$ , lying along the twofold axes of the unit cell. The dimeric unit involves four bridging ligands, each platinum atom being surrounded by four sulfur atoms in a square-planar arrangement. The Pt-Pt distance in the dimer is 2.677 (2) Å, 0.21 Å shorter than the distance between the centers of the  $\text{S}_4$  planes. The  $[\text{PtS}_4]$  square is twisted by  $\sim 21^\circ$  from the eclipsed structure. The Pt-I distances are respectively 2.975 (1) and 2.981 (3) Å, and all the platinum and iodine atoms lie perfectly on the twofold axes of the unit cell. The shorter intradimer distance in this compound compared to that for the unoxidized complex involves only a slight change in the Pt-S distances and the ligand structural parameters.<sup>5</sup> It is of interest to compare the Pt-Pt distance in the oxidized and

**Table IV.** Average Distances (Å) and Angles (deg) in Platinum Complexes

compd	M-M	M-S	C-S	C-C	$\angle\text{SCS}$	$\angle\text{MSC}$
$\text{Pt}_2(\text{dta})_4^a$	2.767 (1)	2.317 (4)	1.68 (2)	1.53 (2)	129.5 (8)	110.5 (5)
$\text{Pt}_2(\text{dta})_4\text{I}$	2.677 (2)	2.324 (6)	1.68 (2)	1.52 (3)	128.1 (11)	109.6 (7)

<sup>a</sup> Reference 5.

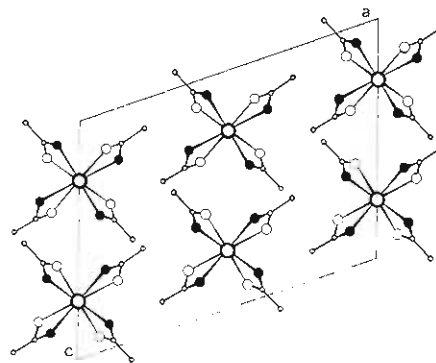


**Figure 2.** Atomic arrangement of  $\text{Pt}_2(\text{CH}_3\text{CS}_2)_4\text{I}$  projected along the  $b$  axis.

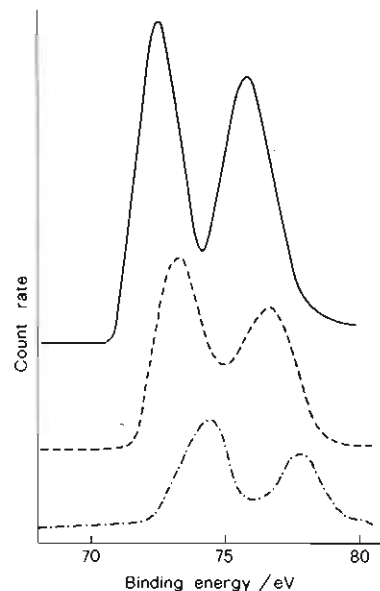


**Figure 3.** X-ray photoelectron spectra of  $\text{Pt}_2(\text{CH}_3\text{CS}_2)_4$  (—),  $\text{Pt}_2(\text{CH}_3\text{CS}_2)_4\text{I}$  (---), and  $\text{Pt}_2(\text{CH}_3\text{CS}_2)_4\text{I}_2$  (-·-·-) in the Pt 4f region.

unoxidized materials. The iodination brings about a significant contraction in the Pt-Pt distance (see Table IV), and this distance should be even shorter in the 1:1 Pt-I complex, where the Pt formal oxidation state is +3.

**X-ray Photoelectron Spectra.** Figure 3 presents  $4f_{7/2}$ ,  $4f_{5/2}$  spectra of  $\text{Pt}_2(\text{CH}_3\text{CS}_2)_4$ ,  $\text{Pt}_2(\text{CH}_3\text{CS}_2)_4\text{I}$ , and  $\text{Pt}_2(\text{CH}_3\text{CS}_2)_4\text{I}_2$ ; the data are listed in Table V. A charging effect was observed, and the values reported are corrected to the C 1s 285.0-eV band. The most important observation made is that the platinum atoms are all equivalent. The full width at half-maximum (fwhm),  $\sim 2.0$  eV, is the same for all the compounds, and this value is comparable to that found for  $\text{K}_2\text{PtCl}_4$ , used as the standard, where all the platinum atoms are equivalent. There is an appreciable shift,  $\sim 2$  eV, in the binding energies, in going from the unoxidized compound to the most oxidized one. The present results are quite consistent with the structural data and give quantitative information on the metal oxidation states in the complexes.

**Mass Spectra.** The mass spectra of  $\text{Pt}_2(\text{CH}_3\text{CS}_2)_4\text{I}_2$  and  $\text{Pt}_2(\text{CH}_3\text{CS}_2)_4\text{I}$  are listed in Table VI. From these data it is clear that they have the same Pt-containing ions although they do not have the same intensity, differing only in the

**Table V.** Electron Binding Energies of Various Platinum Dithioacetato Derivatives<sup>a</sup>

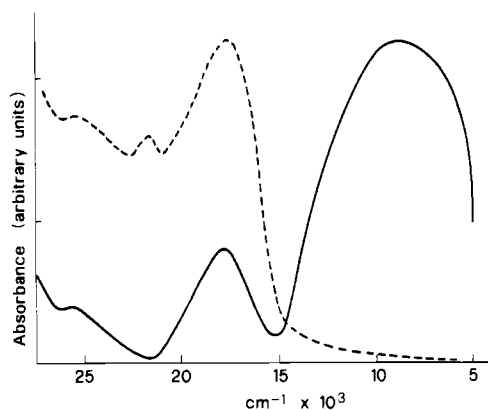
compd	Pt 4f		halogen	ligand S 2p <sup>b</sup>
	5/2	7/2		
Pt <sub>2</sub> (CH <sub>3</sub> CS <sub>2</sub> ) <sub>4</sub>	75.80 (1.8)	72.50 (1.8)		163.60
Pt <sub>2</sub> (CH <sub>3</sub> CS <sub>2</sub> ) <sub>4</sub> I	76.50 (2.1)	73.20 (2.0)	630.8, 619.2	163.50
Pt <sub>2</sub> (CH <sub>3</sub> CS <sub>2</sub> ) <sub>4</sub> I <sub>2</sub>	77.70 (2.0)	74.35 (2.0)	630.6, 619.1	163.70
Pt <sub>2</sub> (CH <sub>3</sub> CS <sub>2</sub> ) <sub>4</sub> Br <sub>2</sub>	77.75 (1.9)	74.25 (2.0)	189.1, 182.0	163.65
Pt <sub>2</sub> (CH <sub>3</sub> CS <sub>2</sub> ) <sub>4</sub> Cl <sub>2</sub>	78.00 (2.4)	74.80 (2.4)	200.0, 198.8	163.60

<sup>a</sup> Energies in eV; full width at half-maximum, fwhm, are in parentheses. <sup>b</sup> Broad peaks.

**Table VI.** Mass Spectra of Pt<sub>2</sub>(CH<sub>3</sub>CS<sub>2</sub>)<sub>4</sub>I<sub>x</sub> (x = 1, 2)<sup>a</sup>

ion	Pt <sub>2</sub> (CH <sub>3</sub> CS <sub>2</sub> ) <sub>4</sub> I <sub>2</sub>		Pt <sub>2</sub> (CH <sub>3</sub> CS <sub>2</sub> ) <sub>4</sub> I	
	m/e	RI	m/e	RI
I <sup>+</sup>	127	74	127	30
HI <sup>+</sup>	128	79	128	50
I <sub>2</sub> <sup>+</sup>	254	67	254	6
PtCH <sub>3</sub> CSS <sup>+</sup>	286	10	285	5
Pt(CH <sub>3</sub> CSS)S <sup>+</sup>	318	6	318	5
Pt(CH <sub>3</sub> CSS)CCS <sup>+</sup>	343	5	343	4
Pt(CH <sub>3</sub> CSS) <sub>2</sub> <sup>+</sup>	377	100	377	100
Pt(CH <sub>3</sub> CSS) <sub>2</sub> S <sup>+</sup>	409	1	410	1
Pt <sub>2</sub> (CH <sub>3</sub> CSS)S <sup>+</sup>	512	5	511	5
Pt <sub>2</sub> (CH <sub>3</sub> CSS)CHS <sup>+</sup>	525	3	524	2
Pt <sub>2</sub> S <sub>4</sub> C <sub>2</sub> <sup>+</sup>	540	3	538	5
Pt <sub>2</sub> (CH <sub>3</sub> CSS)S <sub>2</sub> <sup>+</sup>	545	3	544	5
Pt <sub>2</sub> (CH <sub>3</sub> CSS) <sub>2</sub> <sup>+</sup>	571	5	571	5
Pt <sub>2</sub> (CH <sub>3</sub> CSS) <sub>2</sub> S <sup>+</sup>	603	3	603	3
Pt <sub>2</sub> (CH <sub>3</sub> CSS) <sub>4</sub> <sup>+</sup>	754	5	754	10

<sup>a</sup> The 15 most intense peaks are reported. For the platinum-containing ions the experimental observed isotope abundances have been compared with the theoretical relative intensity histogram generated by the PEEKS QCPE program.

**Figure 4.** Diffuse-reflectance spectra of Pt<sub>2</sub>(CH<sub>3</sub>CS<sub>2</sub>)<sub>4</sub>I<sub>2</sub> (---) and Pt<sub>2</sub>(CH<sub>3</sub>CS<sub>2</sub>)<sub>4</sub>I (—).

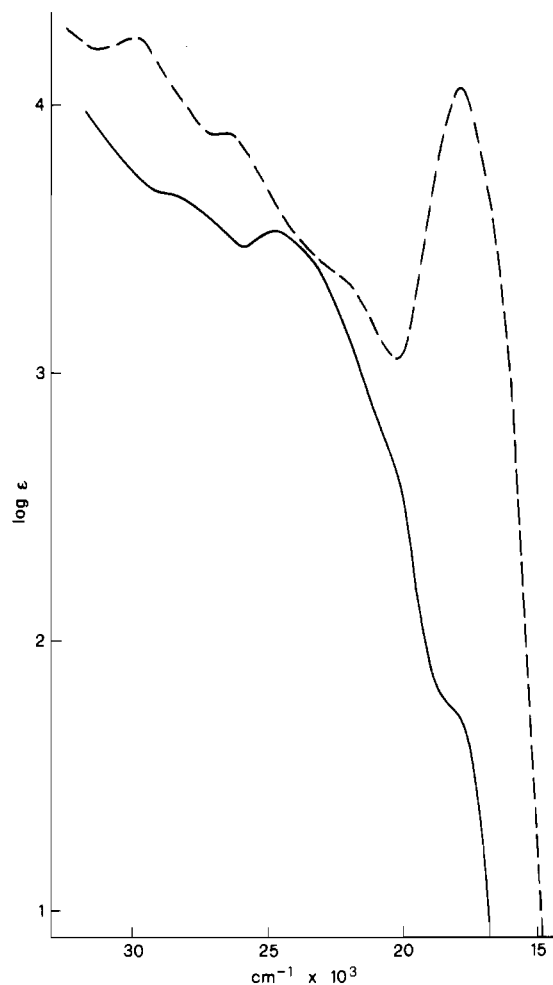
content of the fragment I<sub>2</sub><sup>+</sup>. The reported *m/e* ratios refer to the most intense peak, which corresponds to the monomer Pt(CH<sub>3</sub>CS<sub>2</sub>)<sub>2</sub><sup>+</sup>. Similar fragmentation for Pt-containing ions has been observed previously in the unoxidized Pt<sub>2</sub>(CH<sub>3</sub>CS<sub>2</sub>)<sub>4</sub>.<sup>5</sup> The other complexes, Pt<sub>2</sub>(CH<sub>3</sub>CS<sub>2</sub>)<sub>4</sub>X<sub>2</sub>, where X = Cl, Br, behave like Pt<sub>2</sub>(CH<sub>3</sub>CS<sub>2</sub>)<sub>4</sub>I<sub>2</sub>, except in the X<sub>2</sub><sup>+</sup> fragment, which is absent. In the case of the chloride compound, a fragment corresponding to Pt<sub>2</sub>(CH<sub>3</sub>CS<sub>2</sub>)<sub>4</sub>Cl<sup>+</sup>, *m/e* = 790, has been detected, although with low intensity.

**Electronic Spectra.** Electronic spectral data for Pt<sub>2</sub>(CH<sub>3</sub>CS<sub>2</sub>)<sub>4</sub>X<sub>2</sub> and Pt<sub>2</sub>(CH<sub>3</sub>CS<sub>2</sub>)<sub>4</sub>I are reported in Figures 4 and 5 and Table VII, which also reports the spectra of the related unoxidized tetrakis(dithioacetato)diplatinum(II) described previously<sup>5</sup> for comparison. Upon halogenation of the complex several changes in the spectra are observed. In the solid state (KBr pellets and reflectance) Pt<sub>2</sub>(CH<sub>3</sub>CS<sub>2</sub>)<sub>4</sub>I shows a strong, broad asymmetric absorption band in the near-in-

**Table VII.** Electronic Spectra of Pt<sub>2</sub>(CH<sub>3</sub>CS<sub>2</sub>)<sub>4</sub>X<sub>2</sub> (X = Cl, Br, I) and Pt<sub>2</sub>(CH<sub>3</sub>CS<sub>2</sub>)<sub>4</sub>I

compd	solution <sup>b</sup>	reflectance <sup>c</sup>
Pt <sub>2</sub> (CH <sub>3</sub> CS <sub>2</sub> ) <sub>4</sub> Cl <sub>2</sub>	21.74 (3.30)	21.50
	26.30 <sup>d</sup> (3.63)	24.00 <sup>d</sup>
		26.70 nm <sup>e</sup>
Pt <sub>2</sub> (CH <sub>3</sub> CS <sub>2</sub> ) <sub>4</sub> Br <sub>2</sub>	35.80 (4.60)	
	37.70 <sup>d</sup> (4.57)	
	20.41 (3.57)	20.20
	25.00 <sup>d</sup> (3.53)	23.8 <sup>d</sup>
Pt <sub>2</sub> (CH <sub>3</sub> CS <sub>2</sub> ) <sub>4</sub> I <sub>2</sub>	27.80 (3.92)	27.03 nm
	35.20 (4.66)	
	17.80 (4.07)	17.70
	21.74 (3.31)	21.70
	26.32 (3.90)	25.60 nm
Pt <sub>2</sub> (CH <sub>3</sub> CS <sub>2</sub> ) <sub>4</sub> I	29.60 (4.25)	
	35.09 (4.74)	7.90
		17.70
		25.60

<sup>a</sup> Energies in 10<sup>3</sup> cm<sup>-1</sup> (log ε in parentheses). <sup>b</sup> In dichloromethane. <sup>c</sup> Diluted in MgO. <sup>d</sup> Shoulder. <sup>e</sup> nm = not measured beyond this frequency.

**Figure 5.** Solution spectra of Pt<sub>2</sub>(CH<sub>3</sub>CS<sub>2</sub>)<sub>4</sub>I (—) and Pt<sub>2</sub>(CH<sub>3</sub>CS<sub>2</sub>)<sub>4</sub>I<sub>2</sub> (---) in dichloromethane.

frared region, with a maximum centered at  $7.8 \times 10^3$  cm<sup>-1</sup>. This band is absent in the other halogenated complexes. The estimated molar extinction coefficient is  $\sim 10^4$  M<sup>-1</sup> cm<sup>2</sup>. The band width at half-height,  $\Delta\nu_{1/2}$ , is  $5 \times 10^3$  cm<sup>-1</sup>. Absorption spectra recorded at various temperatures in KBr pellets, between 80 K and room temperature, show only a slight decrease

in the intensity of the band, presumably an indication that it is an electric-dipole-allowed transition. The  $\text{Pt}_2(\text{CH}_3\text{CS}_2)_4\text{X}_2$  complexes are transparent in either the solid state or dichloromethane solution, in the near-infrared region, namely, 700–2000 nm. In solution and in the solid state they show another spectral feature that is evident upon halogenation: in the visible region there is the appearance of new bands at  $17.7 \times 10^3 \text{ cm}^{-1}$  in  $\text{Pt}_2(\text{CH}_3\text{CS}_2)_4\text{I}_2$ , at  $20.4 \times 10^3 \text{ cm}^{-1}$  in  $\text{Pt}_2(\text{C}-\text{H}_3\text{CS}_2)_4\text{Br}_2$ , and at  $21.5 \times 10^3 \text{ cm}^{-1}$  in  $\text{Pt}_2(\text{CH}_3\text{CS}_2)_4\text{Cl}_2$ . These are  $\text{L} \rightarrow \text{M}$  charge-transfer bands, which depend on the halogen present in the compound. Finally, the other spectral feature to be remarked on is the disappearance of the "solid-state effects" shown by  $\text{Pt}_2(\text{CH}_3\text{CS}_2)_4$  and the analogous  $\text{Pt}_2[(\text{CH}_3)_2\text{CHCS}_2]_4$  complexes.<sup>10</sup> This is in agreement with structural data where the columnar structure, responsible for the intermolecular interactions in the unoxidized systems,<sup>11</sup> has been destroyed. Further, the  $nd_{z^2} \rightarrow (n+1)p_z$  transition observed in the dimeric units of the unoxidized systems, in solution, has not been observed.

**Magnetic Properties. (a) Magnetic Susceptibility.** The static magnetic susceptibilities of  $\text{Pt}_2(\text{CH}_3\text{CS}_2)_4\text{X}_2$  ( $\text{X} = \text{I}, \text{Cl}$ ) were measured between 293 and 80 K. They are diamagnetic ( $-7.0 \times 10^{-3} \text{ emu/mol}$ ) as expected for Pt(III) dimers in all the ranges of temperature investigated. The static magnetic susceptibility of  $\text{Pt}_2(\text{CH}_3\text{CS}_2)_4\text{I}$  was measured in the same ranges of temperature, and it gave a constant value of  $-1.3 \times 10^{-4} \text{ emu/mol}$ .

**(b) Electron Spin Resonance.** At liquid  $\text{N}_2$  and at liquid He temperature the EPR spectra of the powdered samples of  $\text{Pt}_2(\text{CH}_3\text{CS}_2)_4\text{I}$  are characterized by a weak single axial signal:  $g_{\perp} = 2.079$  and  $g_{\parallel} = 2.008$ . The spectrum is similar to that reported for the 1-D complex  $\text{K}_2\text{Pt}(\text{CN})_4\text{Br}_{1/3} \cdot 3\text{H}_2\text{O}$ ,<sup>12</sup> for the Pt(IV)-doped Magnus green salt,<sup>13</sup> and for platinum pyridone blue.<sup>14</sup> In contrast with the case for MGS, our compound does not show hyperfine interactions. The same amount of three different samples gave intensities in a 1:2:5:3 ratio. In the case of  $\text{Pt}_2(\text{CH}_3\text{CS}_2)_4\text{X}_2$  compounds no EPR signals were detected.

**Electrical Conductivity.** At room temperature the electrical conductivity of several pellets of different samples of  $\text{Pt}_2(\text{C}-\text{H}_3\text{CS}_2)_4\text{I}$  ranged between  $4 \times 10^{-3}$  and  $7 \times 10^{-3} \Omega^{-1} \text{ cm}^{-1}$ . These data are for compressed polycrystalline samples, and therefore they suffer from interparticle contact resistance effects and from the averaging over all the crystallographic orientations. Nevertheless, they are comparable with those of other similar materials. By comparison with those for other low-dimensional materials, the single-crystal electrical conductivity along the molecular stacking direction should be greater by a factor of  $10^2$ . Variable-temperature studies of electrical conductivity were carried out for several pellets, and a thermally activated charge transport was observed. The apparent activation parameter,  $E_a$ , for two different samples, was obtained by a least-squares fit to the usual relation

$$\sigma = \sigma_0 \exp(-E_a/kT)$$

with  $E_a = 0.05$  and  $0.06 \text{ eV}$ . This equation holds from 77 to 300 K, the temperature range investigated.

## Discussion

$\text{Pt}_2(\text{CH}_3\text{CS}_2)_4\text{X}_2$ . The oxidative addition of halogens to tetrakis(dithioacetato)diplatinum(II) gives complexes with the formula  $\text{Pt}_2(\text{CH}_3\text{CS}_2)_4\text{X}_2$ . They contain platinum atoms in

formal oxidation state +3, and only a few examples of these are known in the literature.<sup>15</sup> The oxidation of the platinum atoms is nicely exemplified by the ESCA data. The Pt 4f binding energies are shifted to higher values with respect to those of the unoxidized systems,<sup>16</sup> while those corresponding to C 1s and S 2p are constant. These complexes are diamagnetic, containing a single metal-metal bond as expected for a  $d^7-d^7$  system with an electronic configuration  $\sigma^2\pi^4\delta^2\delta^*2\pi^{*4}$ .<sup>17</sup>

In the starting material,  $\text{Pt}_2(\text{CH}_3\text{CS}_2)_4$ , the highest occupied orbital,  $\sigma^*$ , is a  $d_{z^2}-d_{z^2}$  antibonding orbital. It follows that the electronic transition  $1a_{2u}(5d_{z^2}) \rightarrow 2a_{1g}(6p_z)$ , in the unoxidized compound, should disappear in the oxidized ones because  $\sigma^*$  is now empty. In fact, in solution, the platinum dithioacetato complex shows a band at  $24.6 \times 10^3 \text{ cm}^{-1}$ , similar to that found in the analogous  $\text{Pd}_2(\text{CH}_3\text{CS}_2)_4$ ,  $25 \times 10^3 \text{ cm}^{-1}$ ,<sup>4</sup> which disappears when the dimeric molecules dissociate into monomers. Further, very recently Crosby et al.<sup>18</sup> assigned the electronic spectrum in a similar diplatinum(II) octaphosphite, containing P–O–P-bridged dimers, on the basis of absorption, fluorescence, and phosphorescence data; they found the  $27.2 \times 10^3 \text{ cm}^{-1}$  band arising from the allowed transition  $1a_{2u} \rightarrow 2a_{1g}$ . In  $\text{Pt}_2(\text{CH}_3\text{CS}_2)_4\text{X}_2$  this band is absent. After oxidation, the Pt–Pt distance in  $\text{Pt}_2(\text{CH}_3\text{CS}_2)_4\text{I}$  decreases (by 0.1 Å), indicating an increase of the metal-metal bond order, after the removal of electrons from the antibonding orbital. This figure is significant if we compare this result with those reported in the literature. Lippard and co-workers showed that there is a correlation between Pt–Pt distances and the formal oxidation state in some platinum blues.<sup>15</sup> We would expect a further contraction of the Pt–Pt distance in  $\text{Pt}_2(\text{CH}_3\text{CS}_2)_4\text{X}_2$  complexes.

$\text{Pt}_2(\text{CH}_3\text{CS}_2)_4\text{I}$ . As reported above, this compound consists of infinite chains of  $\text{---Pt}_2\text{S}_8\text{---I---Pt}_2\text{S}_8\text{---}$  units. The molecular geometry of the  $\text{Pt}_2\text{S}_8$  dimer is similar to that found in unoxidized  $\text{Pt}_2(\text{CH}_3\text{CS}_2)_4$ , while a significant contraction in the Pt–Pt distance is observed, 0.1 Å. Another remarkable feature is the Pt–I distances along the chains. These are almost equal (i.e., 2.975 (1) and 2.981 (3) Å), and the value is intermediate between those for Pt(II)–I, 3.04 Å, and Pt(IV)–I, 2.79 Å.<sup>19</sup> In mixed-valence substances with a singly bridged (halogen) chain, this is quite unusual; in only one case<sup>20</sup> have equal M–X distances been observed. The chain can be formulated as  $[\text{Pt}_2(\text{CH}_3\text{CS}_2)_4\text{I}_2 \cdot \text{Pt}_2(\text{CH}_3\text{CS}_2)_4]_{\infty}$ , where all the Pt atoms are equivalent. The compound is a diamagnetic semiconductor, with an intense, broad, asymmetric band in the near-IR region; at liquid- $\text{N}_2$  temperature there is only a weak EPR signal with no hyperfine structure, the intensity of which varies with the sample preparation. These properties can be rationalized on the basis of a band-structure model. This is justified by inspection of the crystal structure, where the chain can be viewed as being formed of  $[\text{Pt}_2(\text{CH}_3\text{CS}_2)_4]$  and  $[\text{Pt}_2(\text{CH}_3\text{CS}_2)_4\text{I}_2]$  units linked together along one direction, so that the Pt–I distances become nearly equal and the Pt atoms equivalent. Qualitatively, a model elaborated by Hoffmann,<sup>21</sup> based upon the extended Hückel method, and

(10) Bellitto, C.; Dessy, G.; Fares, V.; Flamini, A. *J. Chem. Soc., Chem. Commun.* **1981**, 409.

(11) Day, P. *J. Am. Chem. Soc.* **1975**, *97*, 1588.

(12) Mehran, F.; Scott, B. A. *Phys. Rev. Lett.* **1973**, *31*, 1347.

(13) Mehran, F.; Scott, B. A. *Phys. Rev. Lett.* **1973**, *31*, 99.

(14) Lippard, S. J., et al. *J. Am. Chem. Soc.* **1979**, *101*, 1434.

(15) Hollis, L. S.; Lippard, S. J. *J. Am. Chem. Soc.* **1981**, *103*, 6761.

(16) (a) Nefedov, V. I.; Salyn, Ya. V.; Baranowskii, I. B.; Maiorova, A. G. *Russ. J. Inorg. Chem. (Engl. Transl.)* **1980**, *25*, 116. (b) Bancroft, G. M.; Chan, T.; Puddephatt, R. J.; Brown, M. P. *Inorg. Chim. Acta* **1981**, *53*, L119.

(17) Cotton, F. A. *Acc. Chem. Res.* **1978**, *11*, 225.

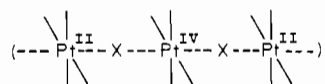
(18) Fordyce, W. A.; Brummer, J. G.; Crosby, G. A. *J. Am. Chem. Soc.* **1981**, *103*, 7061.

(19) Endres, H.; Keller, H. J.; Martin, R.; Hae Nam Gung; Traeger, U. *Acta Crystallogr., Sect. B* **1979**, *B35*, 1885.

(20) Endres, H.; Keller, H. J.; Martin, R.; Notzel, S. *Z. Naturforsch., B: Anorg. Chem., Org. Chem.* **1980**, *35B*, 1274.

(21) Hoffmann, R. *J. Chem. Phys.* **1963**, *39*, 1397.

recently applied by Whangbo<sup>22</sup> to Wolfram's red salt



can, with minor variations, be used to understand the electronic and structural properties of  $\text{Pt}_2(\text{CH}_3\text{CS}_2)_4\text{I}$ . In our compound the interaction can be considered to arise from dimers containing Pt(II) and dimers containing Pt(III), through bridged iodine. The two  $d_{z^2}$  bands are generated by  $\sigma^*$  in  $\text{Pt}_2(\text{CH}_3\text{C-S}_2)_4$ , a doubly occupied orbital, and the same one in  $\text{Pt}_2(\text{C-H}_3\text{CS}_2)_4\text{I}_2$ , a  $\sigma^*$  empty orbital, with a small energy gap,  $E_g$ . The near-IR absorption band can be reasonably assigned as arising from the transitions between these two bands. The temperature dependence of the electrical conductivity gives a very small apparent activation energy, 0.05 eV, which cannot be related to the near-IR band,  $\sim 1$  eV, and therefore the intrinsic band mechanism should be excluded.<sup>23</sup> The electrical conduction then may occur either by an intrinsic "hopping mechanism"<sup>24</sup> or by an extrinsic band-model mechanism. The former seems the more appropriate to describe the conduction

(22) Whangbo, M.; Foshee, M. *J. Inorg. Chem.* **1981**, *20*, 113.

(23) Gutmann, F.; Lyons, L. E. "Organic Semiconductors"; Wiley: New York, 1967; p 19.

(24) Interrante, L. V.; Browth, K. W.; Bundy, F. P. *Inorg. Chem.* **1974**, *13*, 1158.

in our complex. In fact, if we compare our results with those found by Interrante and co-workers<sup>24</sup> on  $\text{M}(\text{NH}_3)_2\text{X}_3$  complexes, where  $\text{M} = \text{Pd}, \text{Pt}$  and  $\text{X} = \text{halogen}$ , we can reasonably suggest this process. In this series of compounds the conductivity is enhanced by pressure and reaches a maximum value as  $\text{M}(\text{II})\text{---X}$  and  $\text{M}(\text{IV})\text{---X}$  distances tend to become equal. The values of the conductivity and the activation parameter at high pressure are comparable with the values reported here, where the Pt-I distances are nearly equal. The EPR signal present in  $\text{Pt}_2(\text{CH}_3\text{CS}_2)_4\text{I}$  could be explained as arising from crystal defects or "impurity centers" with an odd number of electrons along the chain. It is not yet possible to assess their contribution to the electrical conductivity from the data available. Further measurements are needed to elucidate the point.

**Acknowledgment.** We thank Mr. G. Cossu for ESCA measurements, Mr. M. Viola for the assembling of the apparatus for electrical conductivity measurements, Dr. D. Attanasio for helpful discussions, and finally one of the reviewers for his helpful comments.

**Registry No.**  $\text{Pt}_2(\text{CH}_3\text{CS}_2)_4$ , 74868-86-3;  $\text{Pt}_2(\text{CH}_3\text{CS}_2)_4\text{Cl}_2$ , 83897-63-6;  $\text{Pt}_2(\text{CH}_3\text{CS}_2)_4\text{Br}_2$ , 83897-64-7;  $\text{Pt}_2(\text{CH}_3\text{CS}_2)_4\text{I}_2$ , 83897-65-8;  $\text{Pt}_2(\text{CH}_3\text{CS}_2)_4\text{I}$ , 83897-66-9;  $\text{Cl}_2$ , 7782-50-5;  $\text{Br}_2$ , 7726-95-6;  $\text{I}_2$ , 7553-56-2.

**Supplementary Material Available:** A listing of observed and calculated structure factor amplitudes (7 pages). Ordering information is given on any current masthead page.

Contribution from the Departments of Chemistry, University of New Orleans, New Orleans, Louisiana 70148, and Louisiana State University, Baton Rouge, Louisiana 70803

## Synthesis, Molecular Structure, and Magnetic Properties of Some Copper(II) Complexes of Bis(2-pyridylmethyl) Ketazine<sup>1</sup>

CHARLES J. O'CONNOR,<sup>2a</sup> RUDOLFO J. ROMANANCH,<sup>2a</sup> DANIEL M. ROBERTSON,<sup>2a</sup> ETIM E. EDUOK,<sup>2a</sup> and FRANK R. FRONCZEK<sup>2b</sup>

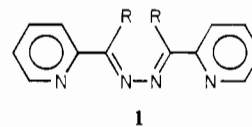
Received May 28, 1982

Two copper(II) complexes of the binucleating ligand bis(2-pyridylmethyl) ketazine (pmk) are reported. The two complexes crystallize with different stereoisomers of the pmk ligand. As a pure solid and in solution the pmk ligand exists as the trans, trans isomer. In the presence of  $\text{Cu}(\text{NO}_3)_2$ , pmk forms a soluble complex, which undergoes a template rearrangement yielding crystals of  $\text{Cu}(\text{cis,trans-pmk})(\text{NO}_3)_2$ . When pmk is dissolved with  $\text{CuCl}_2$ , an insoluble binuclear complex forms without rearrangement of the ligand. The product of  $\text{CuCl}_2$  and pmk has the formula  $\text{Cu}_2(\text{trans,trans-pmk})\text{Cl}_4$ . The magnetic data show very weak antiferromagnetic interactions between the  $\text{Cu}(\text{cis,trans-pmk})(\text{NO}_3)_2$  monomeric units ( $g = 2.22$ ,  $\theta = -1.2$  K). The binuclear complex shows antiferromagnetic intradimer exchange ( $g = 2.10$ ,  $2J = -52$   $\text{cm}^{-1}$ ). Crystal data:  $\text{CuC}_{14}\text{H}_{14}\text{N}_6\text{O}_6$ ,  $M_r = 425.8$ , space group  $C2/c$ ,  $a = 11.356$  (4)  $\text{\AA}$ ,  $b = 17.325$  (5)  $\text{\AA}$ ,  $c = 8.829$  (2)  $\text{\AA}$ ,  $\beta = 91.61$  (3)°,  $Z = 4$ ,  $d_{\text{calcd}} = 1.629$   $\text{g cm}^{-3}$ ,  $\mu(\text{Mo K}\alpha) = 13.6$   $\text{cm}^{-1}$ ,  $R = 0.079$  for 1534 reflections;  $\text{Cu}_2\text{Cl}_4\text{C}_{14}\text{H}_{14}\text{N}_6$ ,  $M_r = 507.2$ , space group  $P2_1/n$ ,  $a = 9.058$  (2)  $\text{\AA}$ ,  $b = 14.115$  (3)  $\text{\AA}$ ,  $c = 14.892$  (3)  $\text{\AA}$ ,  $\beta = 106.26$  (2)°,  $Z = 4$ ,  $d_{\text{calcd}} = 1.843$   $\text{g cm}^{-3}$ ,  $\mu(\text{Cu K}\alpha) = 83.15$   $\text{cm}^{-1}$ ,  $R = 0.055$  for 1911 reflections.

### Introduction

Binuclear metal(II) complexes of azine ligands have been known for several years.<sup>3-12</sup> Complexes of bis(2-pyridyl)

ketazine ligands (**1**,  $\text{R} = \text{H}$ ) with the formula  $\text{M}_2\text{L}_3\text{X}_4$  were



first reported by Stratton and Busch.<sup>3-5</sup> These authors also discussed the subsequent formation of a mononuclear complex of the formula  $\text{ML}_2\text{X}_2$ . In studies of the iron(II) and nickel(II)

(1) Presented at the 183rd National Meeting of the American Chemical Society, Las Vegas, NV, 1982; see Abstracts, No. INOR 112.

(2) (a) University of New Orleans. (b) Louisiana State University.

(3) Stratton, W. J.; Busch, D. H. *J. Am. Chem. Soc.* **1960**, *82*, 4834.

(4) Stratton, W. J.; Busch, D. H. *J. Am. Chem. Soc.* **1958**, *80*, 1286.

(5) Stratton, W. J.; Busch, D. H. *J. Am. Chem. Soc.* **1958**, *80*, 3191.

(6) Stratton, W. J.; Rettig, M. F.; Drury, R. F. *Inorg. Chim. Acta* **1969**, *3*, 97.

(7) Stratton, W. J. *Inorg. Chem.* **1970**, *9*, 517.

(8) Stratton, W. J.; Orgen, P. J. *Inorg. Chem.* **1970**, *9*, 2588.

(9) Andrew, J. E.; Blake, A. B. *J. Chem. Soc. A* **1969**, 1413.

(10) Ball, P. W.; Blake, A. B. *J. Chem. Soc. A* **1969**, 1415.

(11) Dei, A.; Gatteschi, D.; Piergentile, E. *Inorg. Chem.* **1979**, *18*, 89. Benell, C.; Dei, A.; Gatteschi, D. *Ibid.* **1982**, *21*, 1284.

(12) Ghedini, M.; Demunno, G.; Denti, G.; Monotti Lanfredi, A. M.; Tiripicchio, A. *Inorg. Chim. Acta* **1982**, *57*, 87.